Revue de micropaléontologie 70 (2021) 100466

Contents lists available at ScienceDirect

Revue de micropaléontologie

journal homepage: www.elsevier.com/locate/revmic

Micropalaeontological analysis and palaeoenvironmental interpretation of the upper sedimentary sequence of Corinth Marl (Corinth Isthmus, Greece)

Th. Tsourou [a,*], M.V. Triantaphyllou [a], S. Cheilaris [a,b], E.G. Fatourou [a,b], I. Michailidis [a,b], A.P. Nikitas [a,b], M.A. Tzortzopoulou [a,b], M. Dimiza [a], E. Stathopoulou [a]

[a] Faculty of Geology and Geoenvironment, National and Kapodistrian University of Athens, Panepistimioupolis 15784, Athens, Greece
[b] School of Geology, Aristotle University of Thessaloniki, 54124 Thessaloniki, Greece

ARTICLE INFO

Keywords:
Ostracods
Benthic foraminifera
Calcareous nannofossils
Oncoids
Corinth Isthmus
Pleistocene

ABSTRACT

The current study performs a detailed micropalaeontological analysis, in terms of ostracods, benthic foraminifera and calcareous nannoplankton, in order to reconstruct the palaeoenvironmental history of the sedimentary sequence exposed in the central part of Corinth Isthmus. Twenty one samples from two lateral sections were studied, on both sides of a westwards dipping normal fault at the west end of the central horst, which are part of the same stratigraphical sequence. The calcareous nannofossil analysis provided for the first time dating evidence for the upper Corinth Marl sequence, revealing that Section A (at the footwall block of the fault/the upper part of the Corinth Marl) is attributed to the Early Pleistocene /Calabrian (nannofossil biozone MNN19f) and that Section B (at the hanging wall of the fault) is assigned to the Middle Pleistocene /Chibanian (MNN20). Both parts of the studied sequence not only differentiate in age but bear notably separated species composition of the main ostracod assemblages as well. The combined study of ostracod and benthic foraminiferal microfaunas indicated that at least since Early Pleistocene the Corinth Marl deposits at the central part of Corinth Isthmus corresponded to a shallow, restricted, oligohaline lagoon with salinity alternations expressed as layers enriched in nannofossil content. Towards Middle Pleistocene the lagoon presented increased salinity and signs of shoaling. The studied sequence closes upwards with a bed of Middle Pleistocene age, rich in marine molluscs and corals indicating a radical environmental change: the opening of the lagoon and the establishment of a shallow marine coastal environment.

Introduction

Corinth Isthmus is located at the eastern part of the Corinth Gulf (Fig. 1). It is a highly active extensional tectonic environment (Briole et al., 2000) with more than 40 normal and oblique normal faults detected along the Corinth Canal mostly dipping westwards and eastwards from the central horst, towards the Corinth and Saronic Gulfs respectively (Freyberg, 1973; Papanikolaou et al., 2015).

The depositional patterns of the sedimentological sequences in the Corinth Isthmus are of great interest with six transgressive-regressive cycles recognized by Collier (1990) from MIS 11 to MIS 5, whereas preliminary micropalaeontological studies of the Pleistocene and Holocene offshore sequences have been presented by Krstic and Dermitzakis (1981) and Dermitzakis and Triantaphyllou (1990) respectively. Thenceforth, there are so far few detailed palaeoenvironmental studies based on micropalaeontological evidence in the broader area of Corinth deposits (e.g., Papanikolaou et al., 2015; Pallikarakis et al., 2018, 2019).

In this study, we present micropalaeontological records to reconstruct the evolution of the depositional environment in the central part of Corinth Isthmus in order to contribute to the assessment of the relative sea-level change and local tectonic activity influencing the sedimentary sequence. Ostracods and benthic foraminifera constitute a significant part of the studies in coastal regions due to their sensitivity to the environmental variability of the marginal marine environments and especially landlocked and semi-enclosed marine basins (e.g., Triantaphyllou et al., 2003, 2010; Tsourou et al., 2015). Calcareous nannoplankton analysis in certain levels of the studied outcrop aims to provide age constraints to the sedimentary sequence. The depositional history of the studied Corinth Isthmus sediments is completed by a thorough study of a layer made up entirely of oncoids, which is interposed between the marls (Fig. 2).

Study area - geological setting

The eastern part area of the Corinth Isthmus is mainly influenced by four major fault zones (South Alkyonides Fault System, Loutraki, Kechriaie, Agios Vassileios faults), but also by shorter local faults (Papanikolaou et al., 2015; Pallikarakis et al., 2018). As a result of the intense tectonic activity, the area is constantly uplifting and the uplift rate have been estimated approximately at

* Corresponding author.
E-mail address: ttsourou@geol.uoa.gr (T. Tsourou).

http://doi.org/10.1016/j.revmic.2020.100466

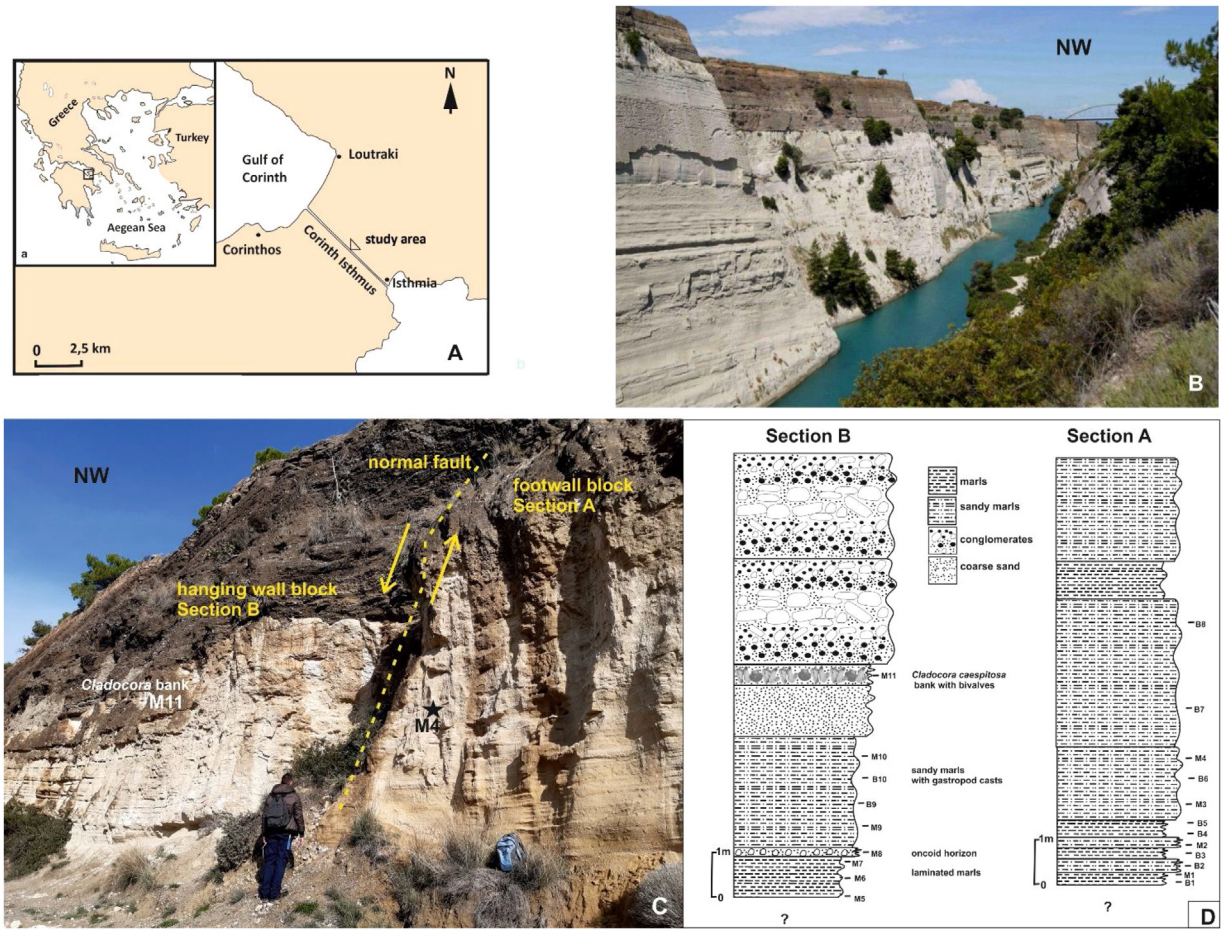

Fig. 1. A. Location of the study area. B. General view, towards west, of the Corinth Canal outcrops faulted by normal faults. C. The under study sedimentary sequence of Corinth Marl. Position of samples M4 and M11 are indicated. D. The lithostratigraphic columns of sampled sections A and B in the central part of Corinth Isthmus.

Fig. 2. A, B. The detected layer rich in oncoids along the Corinth Isthmus section (dashed lines). Its thickness decreases westwards, ending on the forehead of a palaeocliff. C. Detail of the layer with oncoids.

0.3 mm/yr the last 200 kys (Collier et al., 1992; Dia et al., 1997). The continuous uplift of the area as well as sea level changes have had a significant impact on the sedimentology and the sedimentation rate of the Corinth Isthmus. Freyberg (1973) was the first to present the sedimentary sequences of the Corinth Isthmus and pointed the role of sea level changes to the sedimentary facies' alternations in the area. He identified two marine to freshwater cycles of Pleistocene age at the central part of Corinth Isthmus which were later attributed by Collier (1990) to the Corinth Marl.

The term "Corinth Marl" was attributed by Freyberg (1973) to the outcrops of the central horst block, which represent the oldest sediments

exposed in the canal section (Collier, 1990). Above these marly deposits, Collier (1990) described the "first subsequence", which consists of conglomerates and sandy layers and corresponds to the "Hauptkonglomerat" of Freyberg (1973). Additionally, Collier (1990) described the sedimentary facies of the Corinth Marl and in combination with the presence of molluscan fauna in certain levels he presented the upwards transition from freshwater/brackish facies to sediments of a marine environment and suggested an age older than 350 kys.

Collier (1990); Gawthorpe et al. (1994) and McMurray and Gawthorpe (2000) particularly focused in describing sedimentary facies of the broader area, while Collier (1990) distinguished six transgressive subsequences in the Corinth canal area, which include marls, sandstones and conglomerates, and these subsequences are bounded by unconformity surfaces.

Materials and methods

Sampling

The study area is located at the central part of Corinth Isthmus and includes the sedimentary sequence exposed at about 70 m elevation along the north side of the Corinth Canal (Fig. 1). It belongs to the upper part of the so called Corinth Marl formation. In total 21 samples have been collected from the Corinth Isthmus sequence. Sampling has been carried out in two lateral sections on either side of a westwards dipping normal fault at the west end of the central horst (Fig. 1). Both sections are part of the same stratigraphical sequence that the fault broke apart, with Section B to constitute the upper part of the sequence.

Section A is located at the footwall block of the fault. It consists of 10 m alternating beige marls and yellowish sandy marls belonging to the upper part of the Corinth Marl formation.

Section B is located at the hanging wall of the fault (Fig. 1). The sequence consists of two different lithological units from the bottom to the top: about 5 m of beige marls and yellow sandy marls and about 5 m of sandstones and conglomerates (the "Hauptkonglomerat" after Freyberg, 1973). The marls constitute the uppermost part of the Corinth Marl formation. Both two units are bounded by an unconformity surface. On this surface a prominent palaeocliff approximately 1.75 m high, was observed and interpreted as evidence of subaerial exposure (McMurray and Gawthorpe, 2000). Just below the unconformity, the marly sequence ends up with a sandy bed rich in *Cladocora caespitosa* stems and bivalves (sample M11, Fig. 1), dated with IcPD technique on bivalve *Pecten* specimens at >350 kys by Pierini et al. (2016), which is in accordance with the definition of MIS11 at the same point by Collier (1990).

Calcareous nannofossils

In total 2 samples have been examined for the calcareous nannofossil content. A small amount of sediment (~1 mg) per sample has been dissolved in buffered solution and filtered on Whatman cellulose nitrate filters (47 mm diameter, 0.45 μm pore size) using a vacuum filtration system. The filters were open dried and stored in plastic petri dishes. A piece of each filter approximately $8 \times 8\ mm^2$ was attached to a copper electron microscope stub using a double-sided conductive adhesive tape and coated with gold. The filter pieces were examined using a Jeol JSM 6390 SEM (Faculty of Geology and Geoenvironment, National and Kapodistrian University of Athens). A working magnification of 1200× was used throughout the analysis. The nannofossil study was performed on the counts of 300 placoliths per sample (e.g. Thierstein et al., 1977; Triantaphyllou, 2015). The biostratigraphic analysis was based on the biozonal schemes of Rio et al. (1990); Raffi et al. (2006) and Backman et al. (2012).

Ostracods and benthic foraminifera

A total of 21 samples were collected from the marls and the *C. caespitosa* bed for micropalaeontological analysis. The samples were disaggregated in a 5% H_2O_2 solution, washed over 0.125 mm mesh sieves and the residues were oven-dried at approximately 40 °C. Twenty samples bore rich micropaleontological content, while sample M8 was barren.

In most of the cases the specimen abundance was too high and aliquots of the dried material were examined using an Otto microsplitter, in order to retrieve 300 ostracod valves per sample. Complete carapaces were counted as two valves. Benthic foraminifera were rare and in many cases not well preserved. When feasible, 200 benthic foraminifera were obtained from the splitted fraction. The taxa absolute abundances for both groups of microfossils was expressed in number of valves/specimens per 1 g of dry residue.

Both ostracods and benthic foraminifers were identified and photographed by using Leica stereomicroscopes and scanning electron microscope (Jeol JSM 6390; Faculty of Geology and Geoenvironment, National and Kapodistrian University of Athens).

The identification of ostracod species was based mainly on Krstic and Dermitzakis (1981); Mostafawi (1994); Danatsas (1994); Fernandez-Gonzalez et al. (1994); Guernet et al. (2003). Benthic foraminifera specimens were identified according to the generic classification of Loeblich and Tappan (1988, 1994) and the standardized nomenclature of the World Register of Marine Species (WoRMS, 2014). Specimens were considered transported when showing scarce presence and bad state of preservation.

Shannon-Wiener diversity index [H(s)] and the Dominance (D) were also calculated for the ostracod assemblages using PAST 2.12 software package (Hammer et al., 2001). Distribution diagrams were constructed for the most abundant ostracod taxa and the benthic foraminifera assemblages.

Ostracods are usually more abundant than benthic foraminifera in the freshwater to marine transitional environments, especially the oligohaline ones. They are usually present in these environments with oligospecific faunas but with a great number of individuals (e.g. Tsourou et al., 2015). On the contrary, benthic foraminifera present richer and more diversified faunas in the marine environment (e.g. Koukousioura et al., 2012). Commonly, both groups are studied together, as the palaeoecological data retrieved from each group usually complement each other (e.g. Carboni et al., 2002; Cearreta et al., 2003; Triantaphyllou et al., 2003, 2010; Barbieri and Vaiani, 2018). In order to quantify this observation, a ratio between ostracods and benthic foraminifera has been calculated for each sample: O/BFO/(O + BF) x100 were O is the number of ostracod valves per 1 g of sediment and BF is the number of benthic foraminifera individuals per 1 g of sediment.

Q-mode hierarchical cluster analysis was performed (utilizing Ward's method, Euclidean distance) in order to group samples with similar ostracod fauna. Only ostracod species exceeding 3% were taken into account.

Oncoids

Coated grains (spherical to sub spherical nodules) within sample M8 were studied in means of mineralogy, qualitative and semi-quantitative chemical analysis and internal grain structure, by Scanning Electron Microscopy (SEM) combined with X-ray Microanalysis (EDS). The samples were embedded in epoxy resin, sectioned perpendicularly, grinded with SiC powder and polished with diamond paste and cloths. Then, they were coated with carbon in order to allow for accurate micro-analyses with a JEOL JSM-5600 Scanning Electron Microscope, connected to an OXFORD LINK™ ISIS™ 300 X-Ray microanalysis system (Energy Dispersive X-ray Microanalysis-EDS). The sample were analyzed with backscattered electrons (BSE).

In addition, an amount of 2 g from sample M8 was prepared for X-ray Diffraction analysis (XRD), for the mineralogical evaluation of the sample. XRD measurements were performed on a SIEMENS D5005 Diffractometer with CuKa radiation at ambient condition. Analysis of the spectra was conducted using the DIFRAC PLUS v2.2 software by Siemens. Samples were prepared and analyzed at the Faculty of Geology and Geoenvironment, National and Kapodistrian University of Athens.

Results

Calcareous nannoplankton

Calcareous nannoplankton specimens have been identified through SEM analysis in two of the studied samples. Both samples (M4 and M11) revealed relatively abundant, well preserved but poorly diversified assemblages.

Sample M4 (Plate 1) was dominated by small *Gephyrocapsa* spp. (medium length 2–2.5 μm). They were consisting more than 90% of the total assemblage, accompanied by few specimens (3%) of normal-sized gephyrocapsids ≥ 4 μm with bridge parallel to the coccolith short axis (*Gephyrocapsa* sp.3 of Rio et al., 1990 = *Gephyrocapsa parallela* Hay and Beaudry, *G. omega* Bukry), *Helicosphaera carteri* (Wallich) Kamptner (3%), holococcoliths *Helicosphaera* HOL *confusus* type (1.5%) and *Calciosolenia brasiliensis* (Lohmann) Young (1.5%).

Sample M11 (Plate 1) presented very abundant small *Reticulofenestra* spp. (mostly *R. parvula,* (Okada & McIntyre) Biekart <3 μm, 80%), accompanied by small gephyrocapsids (10%), Syracosphaera sp. (5%) and Helicosphaera sp. (4%).

Ostracods

Ostracods were the most abundant group in all nineteen samples, dominating the total microfauna (Table 3), except of sample M11 (~24%). A total of 35 ostracod species were identified: 17 species from Section A where 8 of them present participation rates over 3% and 26 species from Section B with 15 are present with relative abundances over 3% (Tables 1a, 1b). The absolute abundances and the relative frequencies of the identified ostracod species for each sample are presented in Tables 1a and 1b.

The application of Q-mode hierarchical cluster analysis grouped the samples into two major clusters: Cluster A, which included all the samples of section A and Cluster B that consisted of all the samples of Section B (Fig. 3).

Ostracod assemblages in Section A were composed mainly of 4 species (Plate 2). *Cyprideis* sp. was the most abundant, present with both noded and un-noded forms in samples B1, M1, M2, while all the other samples bore only un-noded forms. *Candona* species, mainly with *Candona* cf. *C. nobilis* (*C. nobilis* (Snejder) in Freels, 1980 and Danatsas, 1994) were also present with high frequencies in all the samples of the section. *Tyrrhenocythere kaeveri* Danatsas (= *Tyrrhenocythere hellenica* Guernet) was the third most abundant species, while *Loxoconcha friemannae* was constantly present in all the samples of Section A but with low relative abundancies (up to 6.62%) compared to the other three species. H-index fluctuated between 1.165 (M3) and 1.758 (M4).

Ostracod assemblage of Cluster A1 was discriminated from the one of Cluster A2 by changes in the relative abundances of the dominant species. Samples of Cluster A1 were characterized by the higher values of *Candona*

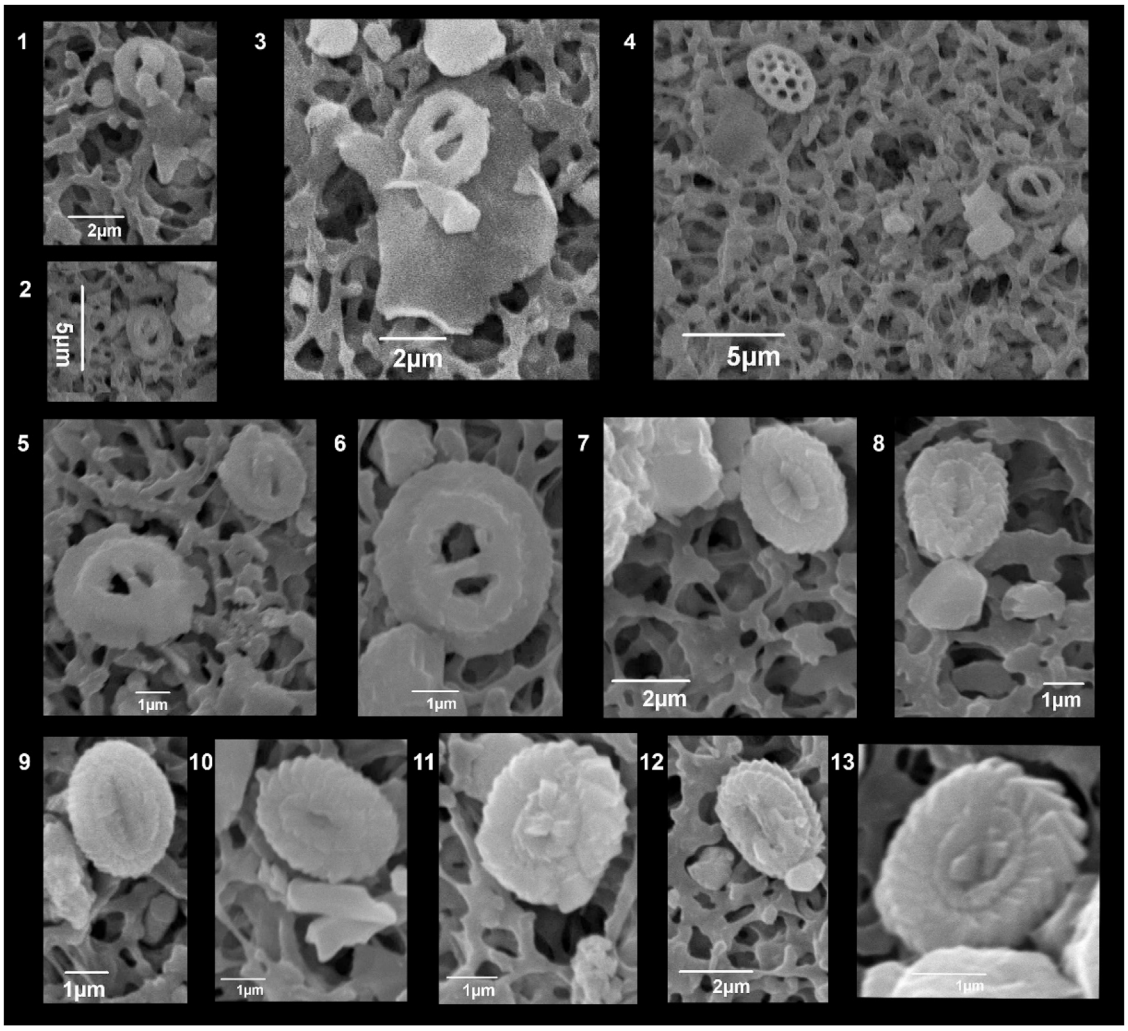

Plate 1. Nannoplankton identified under scanning electron microscopy: **1-3.** Small *Gephyrocapsa* spp. coccoliths, distal view (sample M4), **4.** Holococcolith Helicosphaera HOL confusus type and small *Gephyrocapsa* spp. coccolith, distal views (sample M4), **5.** *Gephyrocapsa* sp.3 (*G. parallela*) coccolith and small *Gephyrocapsa* spp., distal views (sample M4), **6.** *Gephyrocapsa* sp.3 (*G. parallela*) coccolith, distal view (sample M4), **7-10.** *Reticulofenestra parvula* coccoliths, distal views (sample M11). **11-13.** Small *Gephyrocapsa* spp. coccoliths, distal view (sample M11).

Table 1
Absolute **(1a)** and relative **(1b)** frequencies of the ostracod species in the studied samples.

a. valves/ 1 g	B1	M1	B2	B3	M2	B4	B5	M3	B6	M4	B7	B8	M5	M6	M7	M8	M9	B9	B10	M10	M11
Cyprideis torosa (Jones)	0	128	0	0	158	0	0	24	0	39	0	0	212	788	2351	0	1799	3160	4240	218	0
Cyprideis sp.	368	1068	223	980	1248	581	517	773	998	202	1412	1417	0	0	0	0	0	0	0	0	0
Tyrrhenocythere amnicola (Sars)	0	0	0	0	0	0	0	0	0	0	0	0	1304	3520	281	0	5935	1975	4240	390	0
Tyrrhenocythere kaeveri Danatsas	53	228	33	156	190	108	84	114	174	42	272	453	0	0	0	0	0	0	0	0	0
Tyrrhenocythere sp.	0	0	11	31	0	54	0	0	0	0	0	0	0	0	0	0	0	0	0	0	0
Candona neglecta Sars	0	0	0	0	0	0	0	0	0	0	0	0	0	74	447	0	3597	1067	960	218	0
Candona cf. *C. nobilis* (Snejder)	222	53	117	591	237	351	337	192	304	164	510	728	0	0	0	0	0	0	0	0	0
Candona sp.	45	446	19	47	111	41	156	36	43	21	85	118	0	0	0	0	0	0	0	0	0
Euxinocythere schuldtae Mostafawi	0	0	0	0	0	0	0	0	0	0	0	0	0	49	789	0	1919	1027	640	57	0
Euxinocythere sp.	0	0	0	0	0	0	0	0	0	0	0	0	0	25	53	0	899	237	240	19	0
Cytheromorpha sp.	3	24	0	0	16	0	24	0	22	0	0	118	0	0	0	0	0	0	0	0	0
Cyprinotus sp.	0	0	6	0	0	0	24	0	0	6	0	39	0	0	0	0	0	0	0	0	0
Loxoconcha bulgarica Caraion	0	0	0	0	0	0	0	0	0	0	0	0	0	25	182	0	2458	0	0	157	0
L. friemannae Mostafawi	13	33	11	124	142	14	24	48	65	33	102	157	0	0	30	0	839	79	0	4	0
Loxoconcha aff. *L.alata* Brady	0	0	0	0	0	0	0	0	0	0	0	0	0	1428	68	0	540	790	1440	15	0
L. affinis (Brady)	0	0	0	0	0	0	0	0	0	0	0	0	0	0	0	0	0	0	0	0	4
Loxoconcha sp.	3	19	0	0	16	0	12	0	22	12	34	0	0	0	0	0	0	0	0	0	0
Palmoconcha turbida (Mueller)	0	0	0	0	0	0	0	0	0	0	0	0	0	0	0	0	0	0	0	0	17
Xestoleberis cf. *X. dispar* Mueller	0	5	0	0	0	0	0	0	0	0	0	0	16	0	0	0	300	0	80	0	0
X. intermedia Brady	0	0	0	0	0	0	0	0	0	0	0	0	98	123	15	0	3777	119	400	168	0
X. communis Mueller	0	0	0	0	0	0	0	0	0	0	0	0	0	0	61	0	0	0	0	0	5
Leptocythere multipunctata (Seguenza)	0	0	0	0	0	0	0	0	0	0	34	59	0	0	1198	0	60	1067	1680	53	0
L. bacescoi (Rome)	0	0	0	0	32	27	0	6	0	0	0	0	0	0	0	0	60	0	0	0	0
Leptocythere sp.	0	0	0	0	0	0	0	0	0	0	0	0	0	74	106	0	0	0	0	0	0
Aurila convexa (Baird)	0	0	0	0	0	0	0	0	0	24	0	0	0	0	0	0	0	0	0	0	2
Aurila sp.	0	0	0	0	0	0	0	0	0	3	0	0	0	0	0	0	0	0	0	0	4
Cimbaurila cimbaeformis (Seguenza)	0	0	0	0	0	0	0	0	0	3	0	0	0	0	0	0	0	0	0	0	0
Cushmanidea turbida (Mueller)	0	0	0	0	0	0	0	0	0	0	0	0	0	0	68	0	0	0	0	4	0
Hiltermannicythere turbida	0	0	0	0	0	0	0	0	0	0	0	0	0	0	0	0	180	0	0	0	0

(continued on next page)

Table 1 ***(continued)***

a. valves/ 1 g	B1	M1	B2	B3	M2	B4	B5	M3	B6	M4	B7	B8	M5	M6	M7	M8	M9	B9	B10	M10	M11
(Mueller)																					
Cytherois fischeri (Sars)	0	0	0	0	0	0	0	0	0	0	0	0	0	0	0	0	0	79	80	0	0
Semicytherura spp.	0	0	0	0	0	0	0	6	0	3	0	0	0	0	15	0	0	0	0	0	0
Hemicytherura sp.	0	0	0	0	0	0	0	0	0	0	0	0	0	0	0	0	0	0	0	0	1
Callistocythere littoralis (Mueller)	0	0	0	0	0	0	0	0	0	0	0	0	0	0	0	0	0	0	0	0	2
Cytheridea neapolitana Kollmann	0	0	0	0	0	0	0	0	0	0	0	0	0	0	0	0	0	0	0	0	4
Costa edwardsii (Roemer)	0	0	0	0	0	0	0	0	0	0	0	0	0	0	0	0	0	0	0	0	2
total	706	2004	420	1930	2149	1175	1178	1199	1627	551	2449	3089	1630	6105	5664	0	22363	9600	14000	1303	40

b %	B1	M1	B2	B3	M2	B4	B5	M3	B6	M4	B7	B8	M5	M6	M7	M8	M9	B9	B10	M10	M11
Cyprideis torosa (Jones)	0.00	6.40	0.00	0.00	7.35	0.00	0.00	2.00	0.00	7.04	0.00	0.00	13.00	12.90	41.50	0.00	8.04	32.92	30.29	16.71	0.00
Cyprideis sp.	52.07	53.31	53.00	50.80	58.09	49.41	43.88	64.47	61.34	36.74	57.65	45.86	0.00	0.00	0.00	0.00	0.00	0.00	0.00	0.00	0.00
Tyrrhenocythere amnicola (Sars)	0.00	0.00	0.00	0.00	0.00	0.00	0.00	0.00	0.00	0.00	0.00	0.00	79.99	57.66	4.95	0.00	26.54	20.58	30.29	29.90	0.00
Tyrrhenocythere kaeveri Danatsas	7.49	11.37	7.95	8.06	8.82	9.19	7.14	9.50	10.67	7.56	11.11	14.65	0.00	0.00	0.00	0.00	0.00	0.00	0.00	0.00	0.00
Tyrrhenocythere sp.	0.00	0.00	2.65	1.61	0.00	4.60	0.00	0.00	0.00	0.00	0.00	0.00	0.00	0.00	0.00	0.00	0.00	0.00	0.00	0.00	0.00
Candona neglecta Sars	0.00	0.00	0.00	0.00	0.00	0.00	0.00	0.00	0.00	0.00	0.00	0.00	0.00	1.21	7.90	0.00	16.09	11.11	6.86	16.71	0.00
Candona cf. C. *nobilis* (Snejder)	31.44	2.64	27.87	30.63	11.03	29.87	28.60	16.02	18.68	29.75	20.82	23.57	0.00	0.00	0.00	0.00	0.00	0.00	0.00	0.00	0.00
Candona sp.	6.37	22.25	4.53	2.44	5.16	3.49	13.24	3.00	2.64	3.81	3.47	3.82	0.00	0.00	0.00	0.00	0.00	0.00	0.00	0.00	0.00
Euxinocythere schuldtae Mostafawi	0.00	0.00	0.00	0.00	0.00	0.00	0.00	0.00	0.00	0.00	0.00	0.00	0.00	0.81	13.92	0.00	8.58	10.70	4.57	4.40	0.00
Euxinocythere sp.	0.00	0.00	0.00	0.00	0.00	0.00	0.00	0.00	0.00	0.00	0.00	0.00	0.00	0.40	0.94	0.00	4.02	2.47	1.71	1.47	0.00
Cytheromorpha sp.	0.37	1.18	0.00	0.00	0.74	0.00	2.04	0.00	1.33	0.00	0.00	3.82	0.00	0.00	0.00	0.00	0.00	0.00	0.00	0.00	0.00
Cyprinotus sp.	0.00	0.00	1.33	0.00	0.00	0.00	2.04	0.00	0.00	1.08	0.00	1.27	0.00	0.00	0.00	0.00	0.00	0.00	0.00	0.00	0.00
Loxoconcha bulgarica Caraion	0.00	0.00	0.00	0.00	0.00	0.00	0.00	0.00	0.00	0.00	0.00	0.00	0.00	0.40	3.21	0.00	10.99	0.00	0.00	12.02	0.00
L. friemannae Mostafawi	1.87	1.66	2.65	6.45	6.62	1.15	2.04	4.00	4.00	5.94	4.17	5.10	0.00	0.00	0.54	0.00	3.75	0.82	0.00	0.29	0.00
Loxoconcha aff. *L.alata* Brady	0.00	0.00	0.00	0.00	0.00	0.00	0.00	0.00	0.00	0.00	0.00	0.00	0.00	23.39	1.20	0.00	2.41	8.23	10.29	1.17	0.00
L. affinis (Brady)	0.00	0.00	0.00	0.00	0.00	0.00	0.00	0.00	0.00	0.00	0.00	0.00	0.00	0.00	0.00	0.00	0.00	0.00	0.00	0.00	9.58
Loxoconcha sp.	0.37	0.95	0.00	0.00	0.74	0.00	1.02	0.00	1.33	2.16	1.39	0.00	0.00	0.00	0.00	0.00	0.00	0.00	0.00	0.00	0.00
Palmoconcha turbida (Mueller)	0.00	0.00	0.00	0.00	0.00	0.00	0.00	0.00	0.00	0.00	0.00	0.00	0.00	0.00	0.00	0.00	0.00	0.00	0.00	0.00	42.15
Xestoleberis cf. *X. dispar* Mueller	0.00	0.24	0.00	0.00	0.00	0.00	0.00	0.00	0.00	0.00	0.00	0.00	1.00	0.00	0.00	0.00	1.34	0.00	0.57	0.00	0.00
X. intermedia Brady	0.00	0.00	0.00	0.00	0.00	0.00	0.00	0.00	0.00	0.00	0.00	0.00	6.00	2.02	0.27	0.00	16.89	1.23	2.86	12.90	0.00
X. communis Mueller	0.00	0.00	0.00	0.00	0.00	0.00	0.00	0.00	0.00	0.00	0.00	0.00	0.00	0.00	1.07	0.00	0.00	0.00	0.00	0.00	13.41
Leptocythere multipunctata (Seguenza)	0.00	0.00	0.00	0.00	0.00	0.00	0.00	0.00	0.00	0.00	1.39	1.91	0.00	0.00	21.15	0.00	0.27	11.11	12.00	4.10	0.00
L. bacescoi (Rome)	0.00	0.00	0.00	0.00	1.47	2.30	0.00	0.50	0.00	0.00	0.00	0.00	0.00	0.00	0.00	0.00	0.27	0.00	0.00	0.00	0.00
Leptocythere sp.	0.00	0.00	0.00	0.00	0.00	0.00	0.00	0.00	0.00	0.00	0.00	0.00	0.00	1.21	1.87	0.00	0.00	0.00	0.00	0.00	0.00
Aurila convexa (Baird)	0.00	0.00	0.00	0.00	0.00	0.00	0.00	0.00	0.00	4.32	0.00	0.00	0.00	0.00	0.00	0.00	0.00	0.00	0.00	0.00	3.83
Aurila sp.	0.00	0.00	0.00	0.00	0.00	0.00	0.00	0.00	0.00	0.54	0.00	0.00	0.00	0.00	0.00	0.00	0.00	0.00	0.00	0.00	9.58

Table 1 (continued)

b %	B1	M1	B2	B3	M2	B4	B5	M3	B6	M4	B7	B8	M5	M6	M7	M8	M9	B9	B10	M10	M11
Cimbaurila cimbaeformis (Seguenza)	0.00	0.00	0.00	0.00	0.00	0.00	0.00	0.00	0.00	0.54	0.00	0.00	0.00	0.00	0.00	0.00	0.00	0.00	0.00	0.00	0.00
Cushmanidea turbida (Mueller)	0.00	0.00	0.00	0.00	0.00	0.00	0.00	0.00	0.00	0.00	0.00	0.00	0.00	0.00	1.20	0.00	0.00	0.00	0.00	0.29	0.00
Hiltermannicythere turbida (Mueller)	0.00	0.00	0.00	0.00	0.00	0.00	0.00	0.00	0.00	0.00	0.00	0.00	0.00	0.00	0.00	0.00	0.80	0.00	0.00	0.00	0.00
Cytherois fischeri (Sars)	0.00	0.00	0.00	0.00	0.00	0.00	0.00	0.00	0.00	0.00	0.00	0.00	0.00	0.00	0.00	0.00	0.00	0.82	0.57	0.00	0.00
Semicytherura spp.	0.00	0.00	0.00	0.00	0.00	0.00	0.00	0.50	0.00	0.54	0.00	0.00	0.00	0.00	0.27	0.00	0.00	0.00	0.00	0.00	0.00
Hemicytherura sp.	0.00	0.00	0.00	0.00	0.00	0.00	0.00	0.00	0.00	0.00	0.00	0.00	0.00	0.00	0.00	0.00	0.00	0.00	0.00	0.00	1.92
Callistocythere littoralis (Mueller)	0.00	0.00	0.00	0.00	0.00	0.00	0.00	0.00	0.00	0.00	0.00	0.00	0.00	0.00	0.00	0.00	0.00	0.00	0.00	0.00	3.83
Cytheridea neapolitana Kollmann	0.00	0.00	0.00	0.00	0.00	0.00	0.00	0.00	0.00	0.00	0.00	0.00	0.00	0.00	0.00	0.00	0.00	0.00	0.00	0.00	9.58
Costa edwardsii (Roemer)	0.00	0.00	0.00	0.00	0.00	0.00	0.00	0.00	0.00	0.00	0.00	0.00	0.00	0.00	0.00	0.00	0.00	0.00	0.00	0.00	5.75

spp. (27-42%), while *Cyprideis* sp. values fluctuated between 37 and 53% and *T. kaeveri* ranged in between 7 and 9%. Samples of Cluster A2 were marked by the higher participation rates of *Cyprideis* sp. (53-65 %), *Candona* species was present with lower relative abundances (16-25%) and *T. kaeveri* presented relatively higher values (up to 11%).

Ostracod assemblages of the samples grouped at cluster B representing Section B samples and were characterized by higher diversity indices up to 2.073 (M9), lower dominance and increasing participation rates of marine taxa. Clusters B1 and B2 corresponded to two distinctive ostracod associations (Fig. 3; Plate 2).

The association of Cluster B1, which included most of the samples of section B, was marked by the presence of the two most dominant species: *Tyrrhenocythere amnicola* and un-noded *Cyprideis torosa* (Plate 2). These were accompanied mostly by *Candona neglecta*,*Euxinocythere schuldtae*, *Xestoleberis* spp. (*X. intermedia* and *Xestoleberis* cf. *X. dispar*), *Loxoconcha* spp. (*Loxoconcha* aff. *L. alata*, *L. bulgarica*, *L. friemannae*) and *Leptocythere multipunctata*. Several other species were sporadically present in the assemblages with participation rates <1% (Table 1b). The associations at sub-cluster B1a were composed mainly of *T. amnicola* (27-80%), *C. torosa* and *C. neglecta* (up to 17%), *E. schuldtae* (up to 9%), *Loxoconcha* spp. (up to 0-24%) and *Xestoleberis* spp. (2-18%). The associations at sub-cluster B1b were composed mainly of *C. torosa* (30-42%), *T. amnicola* (5-30%), *E. schuldtae* (5-14%), *L. multipunctata* (12-21%), *C. neglecta* (7-11%) and *Loxoconcha* spp. (up to 10%).

The association of Cluster B2 was represented only in sample M11, characterized by low specimen abundance but higher species diversity compared to the samples from the lower, marly part of the section (Cluster B1). The ostracod association consisted of *Palmoconcha turbida*, *Xestoleberis communis*, *Cytheridea neapolitana*, *Aurila* spp., *Callistocythere littoralis*, *Costa edwardsii* and *Hemicytherura* sp.

Benthic foraminifera

Totally 28 benthic foraminiferal species were retrieved from the studied samples. The absolute abundances and the participation rates of the identified foraminiferal species for each sample are presented in Tables 2a and 2b. Samples B6 and M6 were barren of foraminiferal content.

A total of 1–5 species were identified for the majority of the sample, while M3, M4 and M11 presented the highest diversity with 15, 18 and 9 species accordingly. Four samples presented the lower O/BF index: B3 (87%), M3 (71%), M4 (49%) and M11 (24%) but in general foraminifera constituted less than 2% of the total microfauna in most of the samples (Table 3; Fig. 4).

The foraminiferal associations in samples M3, M4 consisted mainly of *Asterigerinata mamilla*, *Elphidium* spp., *Cibicidoides lobatulus* and *Cancris auriculus*, while sample M11 mostly included *A. beccarii*, miliolids, *Elphidium crispum, A. tepida*, and *Cibicidoides lobatulus* (Plate 3).

Oncoids

Sample M8 consisted of oncoids, according to the broader definition given by Flugel (2004). The oncoid grains were generally spheroidal, ellipsoidal and subrectangular in outline with more or less distinct boundaries between the nuclei and the cortex (Plate 4: 3, 4). Typical oncoids (diameter between 2 and 7 mm) (Plate 4: 1), as well as micro-oncoids (diameter between 100 μm and 1 mm) were observed (Plate 4: 2).

The larger and more spheroidal oncoids exhibited nuclei that consist mainly of coralline red algae debris, which based on the characteristic single layers of palisade cells (Plate 4 : 3, 5–8) were attributed mostly to *Lithoporella* sp. (Hills and Jones, 2000; Leszczyński et al., 2012; Richter and Sedat, 1983) (Plate 4: 7, 8). The micro-oncoids, which appeared less spheroidal, contained various types of nuclei such as lithoclasts of quartz, low-Mg calcite, dolomite, filaments, clinochlore, chromite, ankerite,

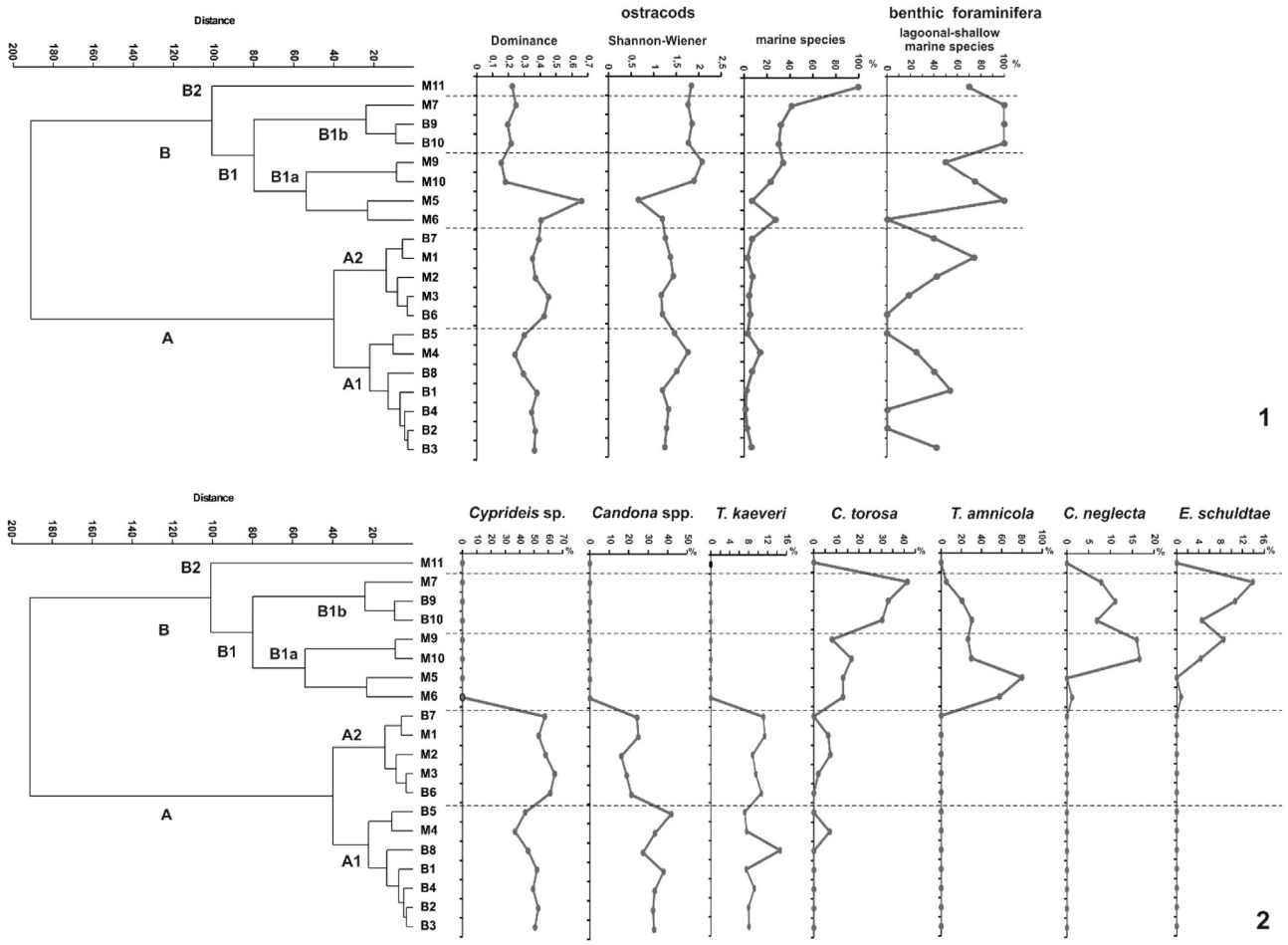

Fig. 3. 1. Q-mode cluster analysis dendrograms, distribution of Shannon-Wiener [H(s)] and Dominance (D) indices and relative abundances of marine ostracod species and lagoonal-shallow marine benthic foraminifera (*Ammonia* spp., *Elphidium* spp., *Haynesina depressula*). **2.** Q-mode cluster analysis dendrograms and relative abundances of the most abundant ostracod species associated with the recorded paleoenvironmental conditions.

minerals of the spinel group, etc. and grains consisting solely of micrite.

In the case of the algal debris oncoids, both nuclei and cortices were determined by XRD to be 100% low-Mg (< 2% Mg) Calcite. The cortex was generally smooth and isopachous and its thickness ranges between 20 and 150 μm in the case of the micro-oncoids and between 500 μm and 1.5 mm in the case of typical oncoids. The number of laminae varied between 1 and 4, but usually the cortex occurred as a crudely layered or massive microcrystalline single coating.

Discussion

Age constraints based on calcareous nannofossils

Despite that calcareous nannoplankton is mostly preserved in pelagic marine sediments (e.g., Perch-Nielsen, 1985; Young, 1994), numerous relatively well preserved coccoliths have been identified in the shallow marine palaeoenvironments identified in samples M4 and M11 (Fig. 4). However, as certain nannoplankton species (e.g., *E. huxleyi*, *Gephyrocapsa* spp., *Reticulofenestra* spp.) are taphonomically resistant to the highly energetic and aggressive conditions between the estuaries and the shelf (e.g., Guerreiro et al., 2005), they have proved to be useful for age determinations in such environments (e.g., Palyvos et al., 2010; Triantaphyllou, 2015; Pallikarakis et al., 2018).

Thus, the calcareous nannoplankton association of sample M4 with dominant small gephyrocapsids and *G. parallela* (up to 2%) places section A deposits within nannofossil biozone MNN19f (Rio et al., 1990) or CNPL10 in between 1.06 and 0.43 Ma (Backman et al., 2012). Taken into account the very low abundance of G. parallela, we suggest that the biostratigraphic assignment of sample M4 is close to the Top absence of Gephyrocapsa (4≥ μm) bioevent at 1.06 Ma (Backman et al., 2012), at MIS 25–27 in the Calabrian (Early Pleistocene); however this needs to be further supported by detailed sampling upwards the section in order to detect any additional marine intrusions within the upper layers of the Corinth Marl. Sample M11 nannofossil assemblage in section B is characterized by very abundant *R. parvula* and the absence of *P. lacunosa*, normal sized gephyrocapsids and *Emiliania huxleyi*. Thus, the biostratigraphic correlation of M11 is likely within, Biozone MNN20 (Rio et al., 1990) or lower part of CNPL11 between 0.43 and 0.29 Ma (Backman et al., 2012) in Middle Pleistocene/Chibanian. This time interval corresponds to sea level highstand MIS7-11 and is in good accordance with the dating of a *Pecten* specimen from exactly the same horizon by IcPD technique as no older than MIS11 (Pierini et al., 2016). Interestingly, the presence of the nannofossil *E. huxleyi* has been detected in the sequences of the eastern part of the Corinth Isthmus, enabling the detection of the sea level highstand MIS 7-5 (Pallikarakis et al., 2018, 2019).

Palaeoenvironmental interpretation

The palaeoenvironmental interpretation resulted from the detailed analysis of the ostracod faunas and the contribution of benthic foraminifera indicates that a shallow brackish lagoon existed in the area of Corinth Isthmus during Early-Middle Pleistocene (Fig. 4). The distribution pattern of the microfaunas points to alternations of oligohaline to oligo-mesohaline waterbodies representing a restricted lagoon with significant fresh water input.

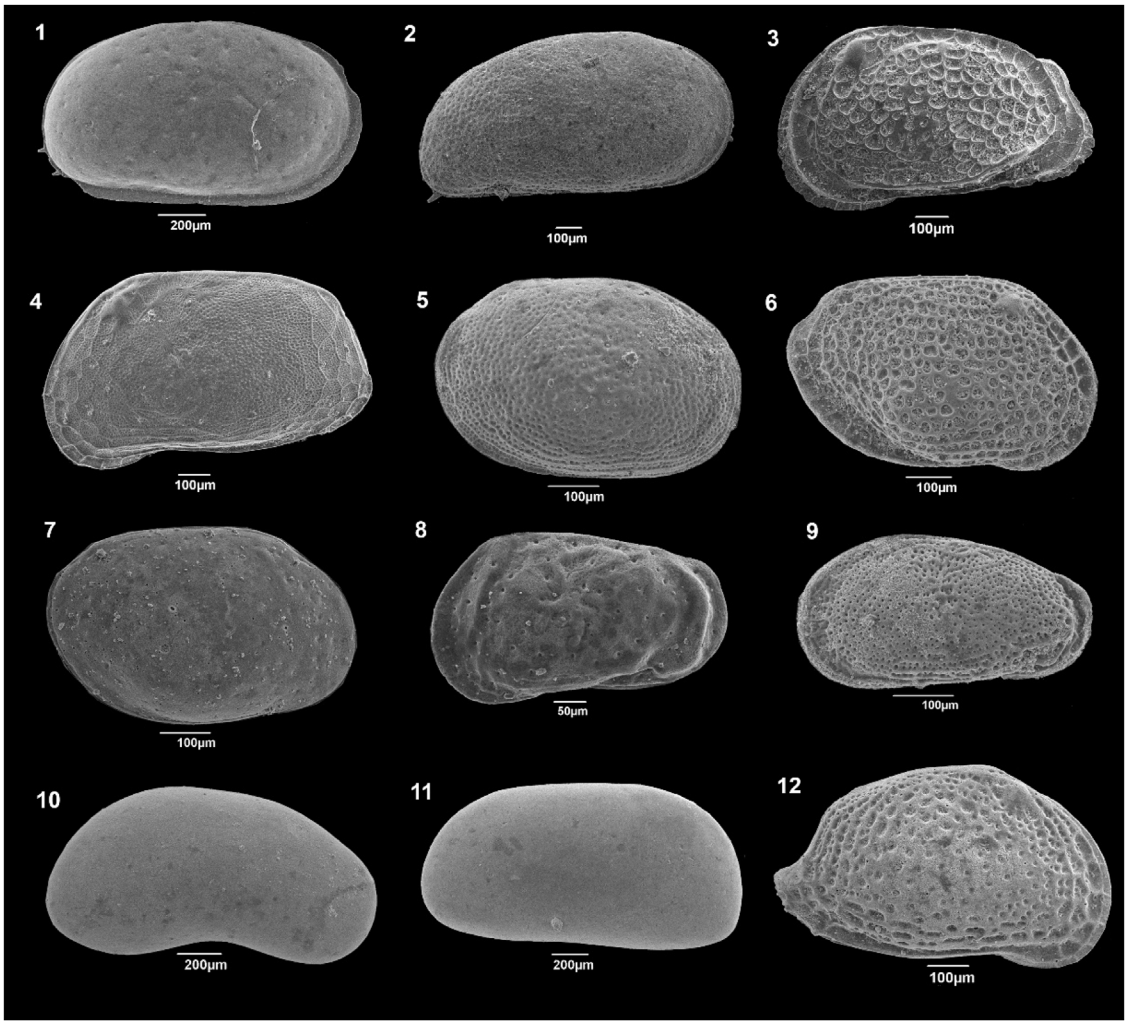

Plate 2. Lateral exterior views of selected ostracod species under scanning electron microscopy. RV: right valve, LV: left valve. **1.** *Cyprideis* sp., RV (sample M3). **2.** *Cyprideis torosa*, RV (sample M10). **3.** *Tyrrhenocythere kaeveri*, LV (sample M1). **4.** *Tyrrhenocythere amnicola*, LV (sample M5). **5.** *Loxoconcha friemannae*, RV (sample M9). **6.** *Loxoconcha* aff. *L. alata*, RV (sample M6). **7.** *Loxoconcha bulgarica,* RV (sample M10). **8.** *Euxinocythere schuldtae*, LV (sample M7). **9.** *Leptocythere multipunctata*, LV (sample M7). **10.** *Candona neglecta*, RV (sample M9). **11.** *Candona* cf. *C. nobilis*, LV (sample M1). **12.** *Aurila convexa*, RV (sample M11).

Section A was characterized by the presence of the ostracod species *Cyprideis* sp., *T. kaeveri* and *Candona* species (*Candona* cf. *C. nobilis* and *Candona* sp.). The genus *Cyprideis* Jones presents high adaptability to brackish environments due to its ecophenotypical plasticity (Ligios and Gliozzi, 2012). For example the species *C. torosa* develops nodes on the valves in very low salinities (Keyser, 2005; Frenzel et al., 2012). The fact that *Cyprideis* sp. presents noded forms in certain layers of Section A is considered as an index of lowering salinity. *Tyrrhenocythere kaeveri* has been reported from brackish deposits of Late Miocene to Pliocene (Danatsas, 1994) and Early Pleistocene in northern Peloponnese (Fernandez-Gonzalez et al., 1994) and Sousaki basin (Papadopoulou et al., 2019). *Tyrrhenocythere* species occur in shallow water environments (depth <30 m) with salinity 5-15‰ and diverse substrates covered by aquatic vegetation (Bronshtein, 1947; Yassini and Ghahreman, 1976; Krstić, 1977). *Candona* species are common in freshwater environments, while some of them tolerate oligo-mesohaline environments (Meisch, 2000; Mazzini et al., 1999; Guernet et al., 2003). *C. nobilis* in particular, has been reported from freshwater and brackish Upper Miocene to Lower Pleistocene deposits in northern Peloponnese (Danatsas, 1994). *L. friemannae* has been described by Mostafawi (1994) from Upper Pleistocene brackish deposits of Northern Peloponnese. The assemblage of cluster A1 with high *Candona* spp. abundance points to an oligohaline environment, while the assemblage of cluster A2 with dominant *Cyprideis* sp. indicates relatively higher salinity of an oligohaline to mesohaline water body.

Concerning benthic foraminifera of Section A (Fig. 3), the scarce presence of the species *Ammonia* spp. and *Elphidium* spp., which are euryhaline taxa common in shallow, brackish and marginal marine environments (Murray, 1991), along with the low diversity and the extremely low participation rates of the foraminiferal species to the total microfauna are in agreement with the restricted brackish environment. At the levels of samples M3, M4 within the Calabrian deposits of section A, temporary sea intrusions took place as indicated by the increased abundance and diversity of benthic foraminifera and the presence of calcareous nannofossil assemblages (sample M4) (Fig. 4).

During Middle Pleistocene (section B) the lagoon had probably a permanent communication with the sea and constant fresh water input. Microfauna characteristic of mesohaline and euhaline shallow and well vegetated environments alternate along the uppermost part of Corinth Marl deposits.

Section B was featured by the prevalence of *T. amnicola*, *C. torosa*, *C. neglecta*, *E. schuldtae*, *Loxoconcha* spp. (mainly *L.* aff *L. alata* and *L. bulgarica*) and *L. multipunctata*. *Tyrrhenocythere amnicola* is a brackish-water species participating in oligohaline to mesohaline assemblages all over the Mediterranean area. In the broader area of Corinth Gulf, it has been described from the Pleistocene of Patras region (Danatsas, 1994; Fernandez-Gonzalez et al., 1994) and Aigion region (Guernet et al., 2003) and from the Upper Pleistocene deposits of northern Peloponnese (Mostafawi, 1994). *Cyprideis torosa* is considered as a species preferring

Table 2
Absolute **(2a)** and relative **(2b)** frequencies of the benthic foraminifera species in the studied samples.

a

specimens/1 g	B1	M1	B2	B3	M2	B4	B5	M3	B6	M4	B7	B8	M5	M6	M7	M8	M9	B9	B10	M10	M11
Ammonia tepida (Cushman)	0	5	0	0	16	0	0	6	0	0	0	0	0	0	83	0	0	40	160	4	8
A. beccari (Linnaeus)	0	0	0	0	32	0	0	0	0	0	0	0	5	0	0	0	180	0	0	4	58
Elphidium crispum (Linnaeus)	5	5	0	0	0	0	0	18	0	48	0	0	0	0	0	0	0	0	0	0	19
E. advenum (Cushman)	0	0	0	47	0	0	0	24	0	9	0	20	0	0	0	0	0	0	0	0	0
E. macellum (Fichtel & Moll)	0	0	0	0	0	0	0	24	0	0	17	0	0	0	0	0	0	0	0	0	0
E. complanatum (d'Orbigny)	0	0	0	78	0	0	0	0	0	78	0	20	0	0	0	0	0	0	0	0	0
E. granosum (d'Orbigny)	0	19	0	0	0	0	0	18	0	9	0	0	0	0	0	0	0	0	0	0	0
Elphidium sp.	0	0	0	0	0	0	0	0	0	0	17	0	0	0	0	0	0	0	0	0	0
Miliolids	0	0	0	0	16	0	0	0	0	0	0	0	0	0	0	0	0	0	0	0	28
Cibicidoides lobatulus (Walker & Jacob)	5	0	0	31	16	0	0	60	0	27	0	39	0	0	0	0	0	0	0	0	6
Cibicides refulgens Montfort	0	0	0	0	0	0	12	24	0	12	0	0	0	0	0	0	0	0	0	0	0
Planorbulina mediterranensis d'Orbigny	0	0	0	0	0	0	0	0	0	0	0	0	0	0	0	0	0	0	0	0	1
Asterigerinata mamilla (Williamson)	0	5	3	124	0	14	0	198	0	188	0	20	0	0	0	0	0	0	0	0	2
Rosalina bradyi (Cushman)	0	0	0	0	0	14	0	12	0	24	34	0	0	0	0	0	180	0	0	0	1
Fissurina sp.	0	0	0	0	0	0	0	0	0	0	0	0	0	0	0	0	0	0	0	4	0
Haynesina depressula (Walker & Jacob)	0	0	0	0	0	0	0	0	0	6	0	0	0	0	0	0	0	0	0	4	0
Nonion sp.	0	0	0	0	32	0	0	0	0	0	0	0	0	0	0	0	0	0	0	0	0
Cancris auriculus (Fichtel & Moll)	0	5	0	16	0	0	0	42	0	66	17	0	0	0	0	0	0	0	0	0	0
Lenticulina orbicularis (d'Orbigny)	0	0	0	0	0	0	0	0	0	3	0	0	0	0	0	0	0	0	0	0	0
Heterolepa dutemplei (d'Orbigny)	0	0	0	0	0	0	0	6	0	6	0	0	0	0	0	0	0	0	0	0	0
Bolivina variabilis (Williamson)	0	0	0	0	0	0	0	12	0	18	0	0	0	0	0	0	0	0	0	0	0
Bolivina sp.	0	0	0	0	0	14	0	0	0	0	0	0	0	0	0	0	0	0	0	0	0
Fursenkoina complanata (Egger)	0	0	0	0	0	0	0	6	0	18	0	0	0	0	0	0	0	0	0	0	0
Reussella spinulosa (Reuss)	0	0	3	0	0	0	0	18	0	18	0	0	0	0	0	0	0	0	0	0	0
Neoconorbina terquemi (Rzehak)	0	0	0	0	0	0	0	18	0	39	0	0	0	0	0	0	0	0	0	0	0
Favulina hexagona (Williamson)	0	0	0	0	0	0	0	0	0	3	0	0	0	0	0	0	0	0	0	0	0
Angulogerina sp.	0	0	0	0	0	0	0	0	0	3	0	0	0	0	0	0	0	0	0	0	0
Textularia agglutinans d'Orbigny	0	0	0	0	0	0	0	0	0	0	0	0	0	0	0	0	0	0	0	0	3
total	11	38	6	296	111	41	12	485	0	573	85	98	5	0	83	0	360	40	160	15	125

b

%	B1	M1	B2	B3	M2	B4	B5	M3	B6	M4	B7	B8	M5	M6	M7	M8	M9	B9	B10	M10	M11
Ammonia tepida (Cushman)	0.00	12.82	0.00	0.00	14.29	0.00	0.00	1.24	0.00	0.00	0.00	0.00	0.00	0.00	100.00	0.00	0.00	100.00	100.00	25.00	6.35
A. beccari (Linnaeus)	0.00	0.00	0.00	0.00	28.57	0.00	0.00	0.00	0.00	0.00	0.00	0.00	100.00	0.00	0.00	0.00	50.00	0.00	0.00	25.00	46.03
Elphidium crispum (Linnaeus)	54.55	12.82	0.00	0.00	0.00	0.00	0.00	3.71	0.00	8.35	0.00	0.00	0.00	0.00	0.00	0.00	0.00	0.00	0.00	0.00	15.08
E. advenum (Cushman)	0.00	0.00	0.00	15.88	0.00	0.00	0.00	4.95	0.00	1.57	0.00	20.20	0.00	0.00	0.00	0.00	0.00	0.00	0.00	0.00	0.00
E. macellum (Fichtel & Moll)	0.00	0.00	0.00	0.00	0.00	0.00	0.00	4.95	0.00	0.00	20.00	0.00	0.00	0.00	0.00	0.00	0.00	0.00	0.00	0.00	0.00
E. complanatum (d'Orbigny)	0.00	0.00	0.00	26.35	0.00	0.00	0.00	0.00	0.00	13.57	0.00	20.20	0.00	0.00	0.00	0.00	0.00	0.00	0.00	0.00	0.00
E. granosum (d'Orbigny)	0.00	48.72	0.00	0.00	0.00	0.00	0.00	3.71	0.00	1.57	0.00	0.00	0.00	0.00	0.00	0.00	0.00	0.00	0.00	0.00	0.00
Elphidium sp.	0.00	0.00	0.00	0.00	0.00	0.00	0.00	0.00	0.00	0.00	20.00	0.00	0.00	0.00	0.00	0.00	0.00	0.00	0.00	0.00	0.00
Miliolids	0.00	0.00	0.00	0.00	14.29	0.00	0.00	0.00	0.00	0.00	0.00	0.00	0.00	0.00	0.00	0.00	0.00	0.00	0.00	0.00	22.22
Cibicidoides lobatulus	45.45	0.00	0.00	10.47	14.29	0.00	0.00	12.37	0.00	4.70	0.00	39.39	0.00	0.00	0.00	0.00	0.00	0.00	0.00	0.00	4.76

Table 2 ***(continued)***

b %	B1	M1	B2	B3	M2	B4	B5	M3	B6	M4	B7	B8	M5	M6	M7	M8	M9	B9	B10	M10	M11
(Walker & Jacob)																					
Cibicides refulgens **Montfort**	0.00	0.00	0.00	0.00	0.00	0.00	100.00	4.95	0.00	2.09	0.00	0.00	0.00	0.00	0.00	0.00	0.00	0.00	0.00	0.00	0.00
Planorbulina mediterranensis **d'Orbigny**	0.00	0.00	0.00	0.00	0.00	0.00	0.00	0.00	0.00	0.00	0.00	0.00	0.00	0.00	0.00	0.00	0.00	0.00	0.00	0.00	0.79
Asterigerinata mamilla **(Williamson)**	0.00	12.82	50.00	41.89	0.00	33.33	0.00	40.82	0.00	32.70	0.00	20.20	0.00	0.00	0.00	0.00	0.00	0.00	0.00	0.00	1.59
Rosalina bradyi **(Cushman)**	0.00	0.00	0.00	0.00	0.00	33.33	0.00	2.27	0.00	4.17	40.00	0.00	0.00	0.00	0.00	0.00	50.00	0.00	0.00	0.00	0.79
Fissurina **sp.**	0.00	0.00	0.00	0.00	0.00	0.00	0.00	0.00	0.00	0.00	0.00	0.00	0.00	0.00	0.00	0.00	0.00	0.00	0.00	25.00	0.00
Haynesina depressula **(Walker & Jacob)**	0.00	0.00	0.00	0.00	0.00	0.00	0.00	0.00	0.00	1.04	0.00	0.00	0.00	0.00	0.00	0.00	0.00	0.00	0.00	25.00	0.00
Nonion **sp.**	0.00	0.00	0.00	0.00	28.57	0.00	0.00	0.00	0.00	0.00	0.00	0.00	0.00	0.00	0.00	0.00	0.00	0.00	0.00	0.00	0.00
Cancris auriculus **(Fichtel & Moll)**	0.00	12.82	0.00	5.41	0.00	0.00	0.00	8.66	0.00	11.48	20.00	0.00	0.00	0.00	0.00	0.00	0.00	0.00	0.00	0.00	0.00
Lenticulina orbicularis **(d'Orbigny)**	0.00	0.00	0.00	0.00	0.00	0.00	0.00	0.00	0.00	0.52	0.00	0.00	0.00	0.00	0.00	0.00	0.00	0.00	0.00	0.00	0.00
Heterolepa dutemplei **(d'Orbigny)**	0.00	0.00	0.00	0.00	0.00	0.00	0.00	1.24	0.00	1.04	0.00	0.00	0.00	0.00	0.00	0.00	0.00	0.00	0.00	0.00	0.00
Bolivina variabilis **(Williamson)**	0.00	0.00	0.00	0.00	0.00	0.00	0.00	2.47	0.00	3.13	0.00	0.00	0.00	0.00	0.00	0.00	0.00	0.00	0.00	0.00	0.00
Bolivina **sp.**	0.00	0.00	0.00	0.00	0.00	33.33	0.00	0.00	0.00	0.00	0.00	0.00	0.00	0.00	0.00	0.00	0.00	0.00	0.00	0.00	0.00
Fursenkoina complanata **(Egger)**	0.00	0.00	0.00	0.00	0.00	0.00	0.00	1.24	0.00	3.13	0.00	0.00	0.00	0.00	0.00	0.00	0.00	0.00	0.00	0.00	0.00
Reussella spinulosa **(Reuss)**	0.00	0.00	50.00	0.00	0.00	0.00	0.00	3.71	0.00	3.13	0.00	0.00	0.00	0.00	0.00	0.00	0.00	0.00	0.00	0.00	0.00
Neoconorbina terquemi **(Rzehak)**	0.00	0.00	0.00	0.00	0.00	0.00	0.00	3.71	0.00	6.78	0.00	0.00	0.00	0.00	0.00	0.00	0.00	0.00	0.00	0.00	0.00
Favulina hexagona **(Williamson)**	0.00	0.00	0.00	0.00	0.00	0.00	0.00	0.00	0.00	0.52	0.00	0.00	0.00	0.00	0.00	0.00	0.00	0.00	0.00	0.00	0.00
Angulogerina **sp.**	0.00	0.00	0.00	0.00	0.00	0.00	0.00	0.00	0.00	0.52	0.00	0.00	0.00	0.00	0.00	0.00	0.00	0.00	0.00	0.00	0.00
Textularia agglutinans **d'Orbigny**	0.00	0.00	0.00	0.00	0.00	0.00	0.00	0.00	0.00	0.00	0.00	0.00	0.00	0.00	0.00	0.00	0.00	0.00	0.00	0.00	2.38

Table 3
The calculated for the ostracod assemblages Shannon-Wiener diversity index and Dominance index and the participation rates of benthic foraminifera and ostracods in the total microfauna.

Samples	Dominance_D	Shannon-Wiener (H)	O/BF = O/(BF + O) %
B1	0.3796	1.193	98.48
M1	0.3518	1.369	98.12
B2	0.3693	1.284	98.63
B3	0.3635	1.243	86.73
M2	0.3697	1.433	95.09
B4	0.3456	1.326	96.68
B5	0.374	1.213	99.00
M3	0.4533	1.165	71.17
B6	0.4247	1.193	100
M4	0.2406	1.758	49.00
B7	0.3915	1.256	96.66
B8	0.2935	1.511	96.90
M5	0.6606	0.6582	99.69
M6	0.4045	1.191	100
M7	0.247	1.76	98.55
M8	–	–	–
M9	0.1546	2.073	98.42
B9	0.1945	1.849	99.59
B10	0.2164	1.767	98.87
M10	0.1806	1.894	98.83
M11	0.2231	1.835	24.15

quiet waters (Carbonel, 1980; Ruiz et al., 2000), being a highly euryhaline species showing adaptability to a wide range of salinities. It occurs in shallow (<30 m) marginal marine environments like lagoons and estuaries and it is found on sediment substrates and on algae (Athersuch et al., 1989). Nevertheless, it is primarily associated with areas of lowered salinity (Athersuch, 1979) and occurs in dense populations when salinity ranges between 2-17‰ (Morkhoven, 1962). *Candona neglecta* is a freshwater species and occurs in temporary and permanent water bodies (Meisch, 2000), but it is also reported from inland and coastal oligohaline brackish waters (Danatsas, 1994; Pavlopoulos et al., 2006; Mazzini et al., 2011). *Euxinocythere schuldtae* was first described by Mostafawi (1994) from upper Pleistocene deposits of Northern Peloponnese and later was also found in upper Pleistocene deposits of Aigion area (Guernet et al., 2003). It is considered as a brackish mostly oligohaline ostracod in associations with *Candona, Cyprideis* and *T. amnicola. Loxoconcha bulgarica* is a Black Sea species that prefers salinities about 11‰ and 5 m depth (Shornikov, 1969) has been described from (?) middle Pleistocene brackish deposits in the channel of Corinth by Krstic and Dermitzakis (1981). *Leptocythere multipunctata* is a shallow marine species (Doruk, 1980) distributed in the Mediterranean since Pliocene (Guernet, 2005). Generally, *Loxoconcha* and *Xestoleberis* species are common marine taxa of the coastal zone and especially *Xestoleberis* species are highly associated with algae (Horne, 1982; Cronin et al., 2001; Triantaphyllou et al., 2003). All above mentioned species constitute the assemblages of the marly part of Section B (cluster B1). The abundance of

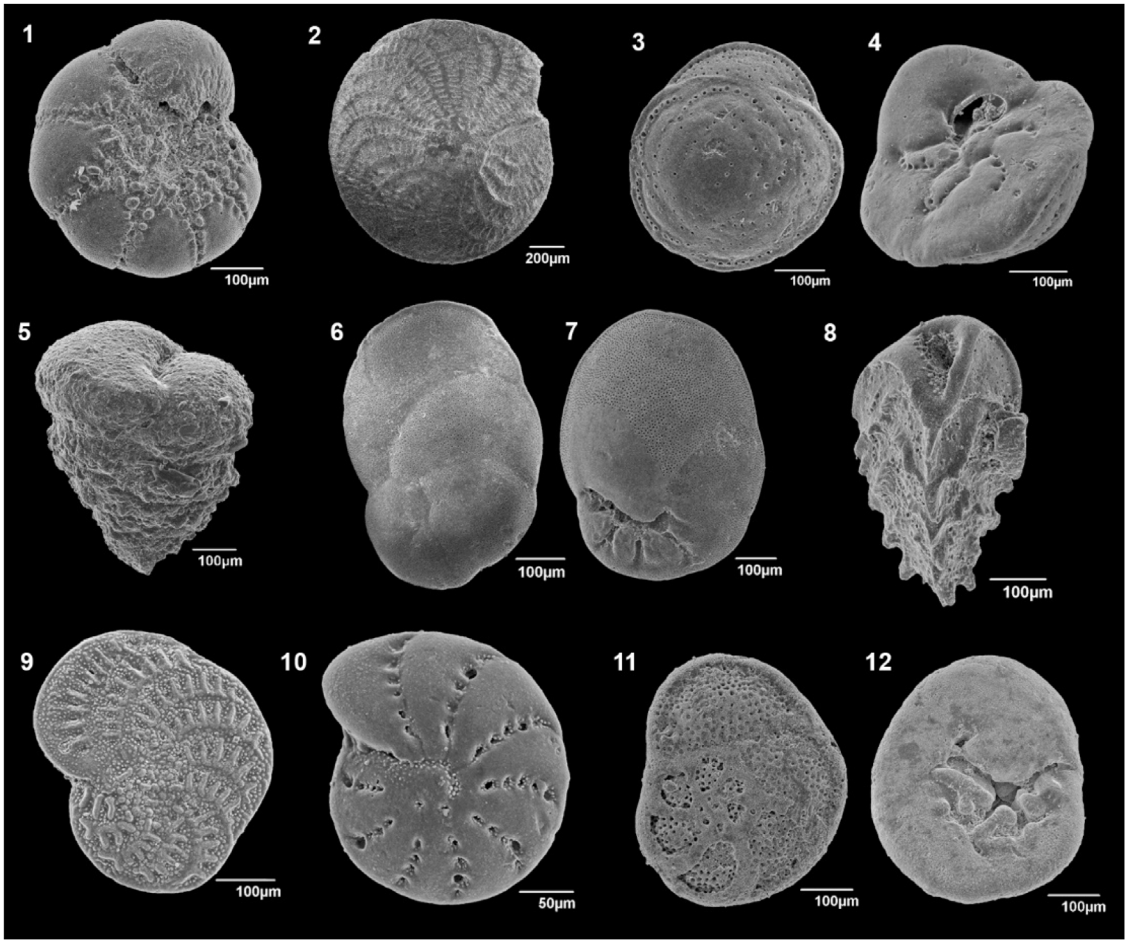

Plate 3. Foraminiferal specimens under scanning electron microscopy: **1.** *Ammonia beccarii*, umbilical side (sample M9). **2.** *Elphidium crispum* (sample M11). **3, 4.** *Asterigerinata mamilla*, 1. spiral side, 2. umbilical side (sample M4). **5.** *Textularia agglutinans* (sample M11). **6, 7.** *Cancris auriculus*, 6. spiral side, 7. umbilical side (sample M4). **8.** *Reusella spinulosa* (sample M4). **9.** *Elphidium complanatum* (sample B3). **10.** *Elphidium advenum* (sample B3). **11, 12.** *Rosalina bradyi*, 11. spiral side, 12. umbilical side (sample M4).

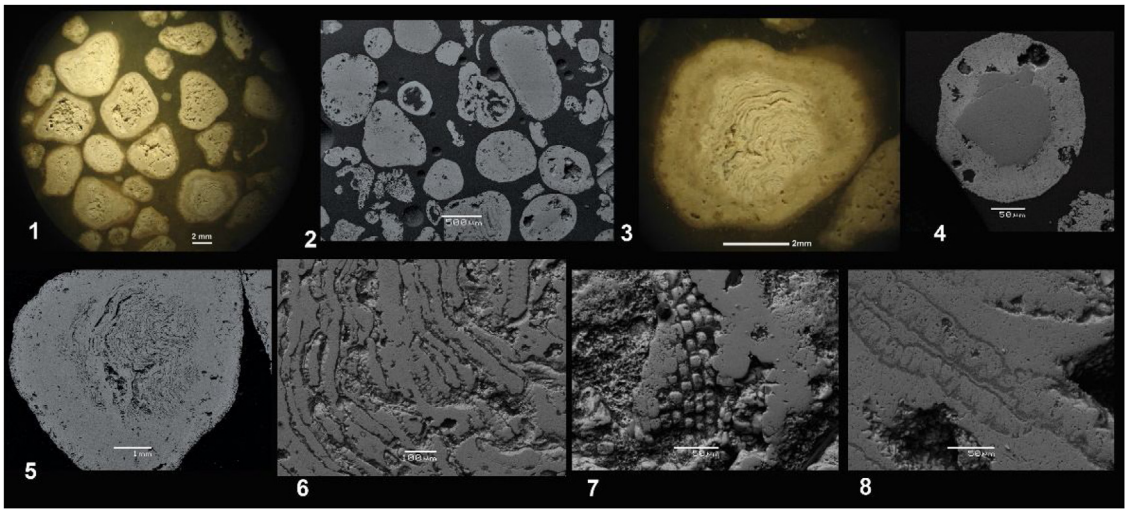

Plate 4. 1, 2. Oncoids (left, stereoscopic view) and micro-oncoids (right, SEM image) from sample M8. **3, 4.** Oncoid with red algae debris nucleus with numerous layers within cortex (left, stereoscopic view), micro-oncoid with a siliceous nucleus (right, SEM image) and an isopachous cortex. **5, 6.** SEM images of an oncoid with red algae debris nucleus (left), detail of algal structure (right). **7, 8.** Details of algal debris attributed to *Lithoporella* sp. Single layers of palisade cells as well as crystals of the microcrystalline low-Mg Calcite are observed (SEM images).

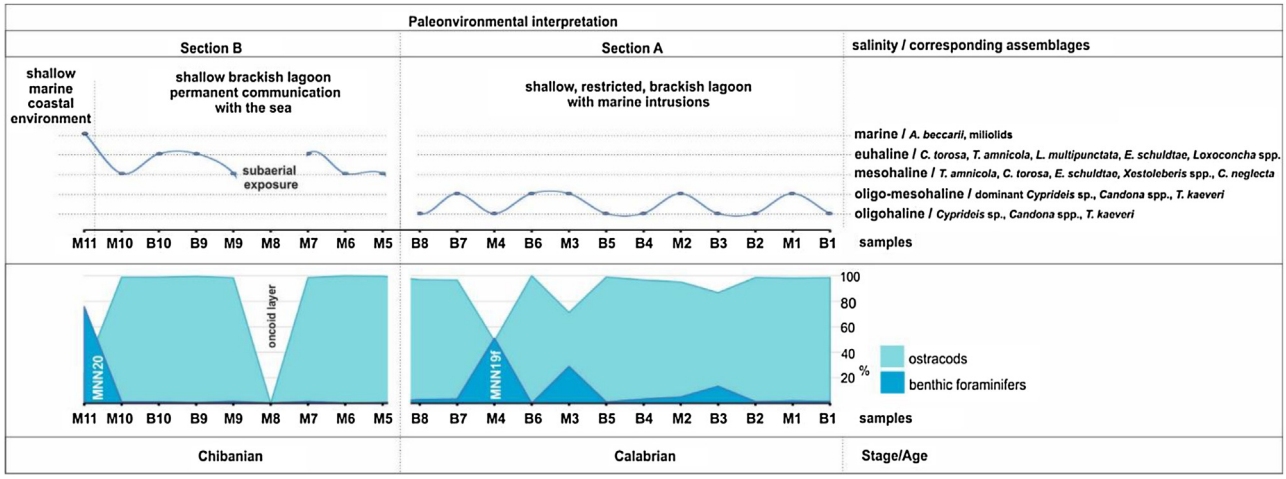

Fig. 4. Palaeoenvironmental interpretation of the upper Corinth Marl based on the participation rates of ostracods and benthic foraminifera in the total microfauna. Increased contribution of benthic foraminifera in the assemblages coincides with marine intrusions, enabling calcareous nannofossil datings.

oligohaline-mesohaline taxa and the increased participation rates of marine species coupled with high diversity, point to a brackish mesohaline-euhaline environment with limited but stable communication with the sea. In particular, the lack of nodded valves in *C. torosa* specimens suggests salinities >7‰ (Frenzel et al., 2012). Samples M5, M6, M9 and M10 (subcluster B1a) present increased freshwater input (higher abundances of *C. neglecta*) and the high presence of *Xestoleberis* spp. along with *C. torosa* and *T. amnicola* point to a shallow high vegetated brackish environment. Samples M7, B9, B10 (subcluster B1b) represent a brackish environment with higher salinity as it is suggested by the relative abundances of *L. multipunctata* and *Loxoconcha* spp.

Concerning benthic foraminifera of Section B (cluster B1; Fig. 3), the assemblages are strongly dominated by *Ammonia* spp. (mainly *A. tepida*. *Ammonia tepida* is commonly reported as opportunistic, tolerant to lower salinities and/or salinity fluctuations in shallow marine, lagoonal and deltaic environments (e.g. Debenay et al., 2005; Frontalini et al., 2009; Koukousioura et al., 2012; Dimiza et al., 2016).

The ostracod association of M11 (cluster B2), which was retrieved from the *C. caespitosa* bank consists entirely of species common in the marine Mediterranean assemblages, indicating a shallow littoral open marine environment (e.g., Bonaduce et al., 1975; Athersuch et al., 1989; Lachenal, 1989; Tsourou, 2012). Accordingly, the benthic foraminifera assemblage of this layer (sample M11) consists mainly of *A. beccarii* and the full marine miliolids (Murray, 1991; Sgarrella and Moncharmont Zei, 1993; Koukousioura et al., 2012).

The oncoid layer at the lower part of section B is of particular interest concerning environmental changes that took place in the studied area. Algal oncoids are regarded as indicators of shallow-water environments with low to medium wave agitation, usually in a back-reef setting, where trapped sediment and skeletal fragments are bound by a microbial biofilm and incorporated by microbially mediated precipitation (Flügel, 2004; Hills and Jones, 2000; Pederson et al., 2015). The oncoids found as a discrete layer in the studied sequence were poorly laminated displayed irregular to subspherical shapes and a less dense, fabric, thus they were probably formed in a very shallow environment, with low to medium wave agitation, in a back reef setting (Pederson et al., 2015). In particular, the presence of an oncoid layer is connected to a progressive shoaling, mostly referring to a depth below 15 m (Hills and Jones, 2000; Richter and Sedat, 1983). The

oncoid layer observed in the uppermost part of Corinth Marl in the studied section B decreases its thickness westwards and the horizon ends laterally on the forehead of a palaeo-cliff (Fig. 2). Hence, the detected oncoid layer could be associated with a disconformity surface due to progressive shoaling (e.g., Pederson et al., 2015) and subaerial exposure; the existence of certain sedimentary features would explain the significant age difference between the two sides of the fault. Similar layers with oncoids have also been reported in the area of the Corinth Gulf, by Richter and Sedat (1983).

Overall, the environmental reconstruction of the uppermost part of Corinth Marl reflects a gradual opening of a shallow lagoon, with the marine transgression that peaks at *C. caespitosa* bank, corresponding to the MIS11 sea level highstand.

The combination of detailed palaeoenvironmental analysis of the upper part of the Corinth Marl and biostratigraphic analysis contributes tothe dating of these deposits and to the understanding of the palaeogeographical evolution of the broader area, providing additional constraints in order to comprehend the uplift of the eastern part of the Corinth Gulf. Existing data on the age of the Corinth Marl sediments are vague, referring to them as of Plio-Pleistocene age in general (e.g. Papanikolaou et al., 2015). The calcareous nannofossil biostratigraphical analysis in this study confirms previous estimations regarding the Middle Pleistocene/Chibanian age of *C. caespitosa* bank (Collier, 1990; Pierini et al., 2016) and defines for the first time the Calabrian stage from deeper horizons of the marly sequence. The detailed and multidisciplinary micropalaeontological analysis of the exposed uppermost part of Corinth Marl at the central part of Corinth Isthmus demonstrated the existence of a shallow oligohaline to oligo-mesohaline lagoon during Early Pleistocene with significant freshwater input, sporadic communication with the sea and marine intrusions. Towards Middle Pleistocene, the marine influence in the lagoon increased and gradually the communication with the sea became permanent indicating sea level rise. At the same time the water depth decreased and the area was temporary subaerially exposed, probably due to the tectonic uplift. Finally, a marine coastal environment was formed corresponding to the warm MIS 11 sea level highstand, which is the lowermost of sea level maxima documented in the exposed part of the Corinth canal sedimentary sequence.

Conclusions

The calcareous nannofossil analysis revealed significant evidence about the age of the upper part of Corinth Marl formation on both sides of a westwards dipping normal fault at the central part of Corinth Isthmus. The footwall block of the fault is attributed to the Early Pleistocene /Calabrian (MNN19f). The hanging wall of the fault represents the uppermost part of the studied sequence and it is attributed to the Middle Pleistocene/ Chibanian (MNN20). Despite that the total thickness of the sequence is not easy to estimate due to the displacement caused by the fault, the age differentiation of the two blocks proves to be quite significant.

The two parts of the studied sequence of the Corinth Marl are not only differentiated in age but also bear notably separated species composition of the main ostracod assemblages with significant similarities between the ostracod assemblages of this study to others around Corinth Gulf.

Micropalaeontological analysis, along with the observed sedimentary facies enabled a detailed palaeoenvironmental interpretation as the distribution patterns of the identified microfaunal assemblages revealed that at least since Calabrian (MNN19f; MIS 25-27) the depositional environment of the central part of Corinth Isthmus corresponded to a shallow, restricted, brackish lagoon with salinity alternations (oligohaline to oligo-mesohaline). Towards Middle Pleistocene the lagoon presented increased salinity (mesohaline to euhaline conditions) pointing to a permanent communication with the sea and at least one episode of shoaling and subaerial exposure.

At the top of the lagoonal deposits, a sandy bed rich in macro- and micro- fossils (MNN20) indicates a radical environmental change: the opening of the lagoon and the establishment of a shallow marine coastal environment within sea level highstand MIS11.

Declaration of interests

The authors declare that they have no known competing financial interests or personal relationships that could have appeared to influence the work reported in this paper.

Acknowledgments

The constructive criticism of the two anonymous reviewers is greatly appreciated. The current research was accomplished in the framework of the IPSP “Palaeontology-Geobiology” (School of Geology, Aristotle University of Thessaloniki; Faculty of Geology and Geoenvironment, National and Kapodistrian University of Athens).

References

Athersuch, J., 1979. The ecology and distribution of the littoral ostracods of Cyprus. J. Nat. Hist. 13, 135–160.
Athersuch, J., Horne, D.J., Whittaker, J.E., 1989. Marine and brackish water Ostracods (Superfamilies Cypridacea and Cytheracea). Synopses of the British Fauna (New Series) 43, 343.
Backman, J., Raffi, I., Rio, D., Fornaciari, E., Pälike, H., 2012. Biozonation and biochronology of Miocene through Pleistocene calcareous nannofossils from low and middle latitudes. Newsl. Stratigr. 45 (3), 221–244.
Barbieri, G., Vaiani, S.C., 2018. Benthic foraminifera or Ostracoda? Comparing the accuracy of palaeoenvironmental indicators from a Pleistocene lagoon of the Romagna coastal plain (Italy). J. Micropalaeontol. 37 (1), 203–230.
Bonaduce, G., Ciampo, G., Masoli, M., 1975. Distribution of Ostracoda in the Adriatic Sea. Pubbl. Staz. Zool. Napoli 40, 1–304.
Briole, P., Rigo, A., Lyon-Caen, H., Ruegg, J.C., Papazissi, K., Mitsakaki, C., Balodimou, A., Veis, A., Hatzfeld, D., Deschamps, A., 2000. Active deformation of the Corinth rift, Greece: results from repeated Global Positioning System surveys between 1990 and 1995. J. Geophys. Res. Solid Earth 105 (B11) 25,605–25,625.
Bronshtein, Z.S., 1947. Fauna SSSR, Rakoobraznye, Tom II, Vypusk 1 Ostracoda presnyh Vod. 370 Pp. Academy of Sciences of the USSR Publishers, Moscow. (English Translation 1988: Freshwater Ostracoda—Fauna of the USSR: Crustaceans, II(1), 455 Pp. AA Balkema, Rotterdam). .
Carbonel, P., 1980. Les ostracodes et leur intérêt dans la définition des écosystèmes estuariens et de la plateforme continentale. Essais d’application à des domaines anciens. Mémoires de l’Institut géologique du Bassin d’Aquitaine 11, 1–350.
Carboni, M.G., Bergamin, L., Di Bella, L., Iamundo, F., Pugliese, N., 2002. Palaeoecological evidences from foraminifers and ostracods on Late Quaternary sea–level changes in the Ombrone river plain (central Tyrrhenian coast, Italy). Geobios, Mémoire special 24, 40–50.
Cearreta, A., Cachão, M., Cabral, M.C., Bao, R., Ramalho, M.J., 2003. Lateglacial and Holocene environmental changes in Portuguese coastal lagoons: 2. Reconstruction of the Santo Andrécoastal area (SW Portugal) during the last 14,000 years based on microfossil multiproxy evidence. Holocene 13, 449–460.
Collier, R.E.L., 1990. Eustatic and tectonic controls upon Quaternary coastal sedimentation in the Corinth Basin. Greece. Journal of the Geological Society 147 (2), 301–314.
Collier, R.E.L., Leeder, R.M., Rowe, P., Atkinson, T., 1992. Rates of tectonic uplift in the Corinth and Megara basins, Central Greece. Tectonics 11, 1159–1167.
Cronin, T.M., Holmes, C.W., Brewster-Wingrad, S., Ishman, S.E., Dowsett, H.J., Keyser, D., Waibel, N., 2001. Historical trends in epiphytal ostracodes from Florida bay: implications for seagrass and macro-benthic algal variability. Bulletins of American Paleontology 361, 159–181.
Danatsas, I., 1994. Jungneogene Ostrakoden aus der NW- und N-Peloponnes (griechenland). Münstersche Forschungen zur Geologie und Paläontologie 76, 97–167.
Debenay, J.-P., Millet, B., Angelidis, M.O., 2005. Relationships between foraminiferal assemblages and hydrodynamics in the gulf of Kalloni. Greece. Journal of Foraminiferal Research 35 (4), 327–343.
Dermitzakis, M.D., Triantaphyllou, M.V., 1990. Ecostratigraphical observations at the eastern part of Corinthiakos Gulf. Annales Geologiques des pays Helleniques 34 (2), 127–161.
Dia, A.N., Cohen, A.S., O’Nions, R.K., Jackson, J.A., 1997. Rates of uplift investigated through 230Th dating in the Gulf of Corinth (Greece). Chem. Geol. 138, 171–184.
Dimiza, M.D., Koukousioura, O., Triantaphyllou, M.V., Dermitzakis, M.D., 2016. Liveand dead benthic foraminiferal assemblages from coastal environmentsof theAegean Sea (Greece): distribution and diversity. Rev. Micropaleontol. 59, 19–32.
Doruk, N., 1980. On *Leptocythere multipunctata* (SEGUENZA). Stereo-Atlas of Ostracod Shells 7, 151–154.
Fernandez-Gonzalez, M., Frydas, D., Guernet, C., Mathieu, R., 1994. Foraminifères et Ostracodes du Pliopléistocène de la région de Patras (Grèce). Intérêt stratigraphique et paléogéographique. Revista Española de Micropaleontología, Madrid XXVI (1), 89–108.
Flügel, E., 2004. Microfacies of Carbonate Rocks: Analysis, Interpretation and Application. Springer, Berlin, pp. 976.
Freels, D., 1980. Limnische Ostrakoden aus dem Jungtertiär und quartär der Türkei. Geologisches Jahrbuch 39, 3–169.
Frenzel, P., Schulze, I., Pint, A., 2012. Noding of *Cyprideis torosa* valves (Ostracoda) – a proxy for salinity? New data from field observations and a long-term microcosm experiment. Int. Rev. Hydrobiol. 97 (4), 314–329.

Freyberg, V., 1973. Geologie Des Isthmus Von Korinth. Erlangen Geologische Ablhandlungen, Heft 95. Junge Und Sohn, Universitats Buchdruckerei Erlangen, 183 Pp. (in German). .
Frontalini, F., Buosi, C., Da Pelo, S., Coccioni, R., Cherchi, A., Bucci, C., 2009. Benthic foraminifera as bio-indicators of trace element pollution in the heavily contaminated Santa Gilla lagoon (Cagliari, Italy). Mar. Pollut. Bull. 58, 858–877.
Gawthorpe, R.L., Fraser, A.J., Collier, R., 1994. Sequence stratigraphy in active extensional basins: implications for the interpretation of ancient basin fills. Mar. Pet. Geol. 11 (6), 642–658.
Guernet, C., 2005. Ostracodes et stratigraphie du Néogène et du Quaternaire méditerranéens ostracodes. Rev. Micropalã©ontologie 48 (2), 83–122.
Guernet, C., Lemeille, F., Sorel, D., Bourdillon, C., Berge-Thierry, C., Manakou, M., 2003. Les ostracodes et le quaternaire d'Aigion (Golfe De Corinthe, Grèce). Rev. Micropalã©ontologie 46, 73–93.
Guerreiro, C., Cachão, M., Drago, T., 2005. Calcareous nannoplankton as a tracer of the marine influence on the NW coast of Portugal over the last 14000 years. Journal of Nannoplankton Research 27 (2), 159–172.
Hammer, O., Harper, D.A.T., Ryan, P.D., 2001. PAST: paleontological statistics software package for education and data analysis. Paleontologia Electronica 4 (1) article 4, 9p.
Hills, D.J., Jones, B., 2000. Peyssonnelid rhodoliths from the late pleistocene ironshore formation, Grand Cayman, british West Indies. Palaios 15 (3), 212–224.
Horne, D.J., 1982. The vertical distribution of phytal ostracods in the intertidal zone at Gore Point, Bristol Channel, U.K. J. Micropaleontol. 1, 71–84.
Keyser, D., 2005. Histological peculiarities of the nodin process in *Cyprideis torosa* (Jones) (Crustacea, Ostracoda). Hydrobiologia 538, 95–106.
Koukousioura, O., Triantaphyllou, M.V., Dimiza, M.D., Pavlopoulos, K., Syrides, G., Vouvalidis, K., 2012. Benthic foraminiferal evidence and paleoenvironmental evolution of Holocene coastal plains in the Aegean Sea (Greece). Quat. Int. 261, 105–117.
Krstić, N., 1977. The ostracod genus *tyrrhenocythere*. In: Löffler, H., Danielopol, D. (Eds.), Aspects of Ecology and Zoogeography of Recent and Fossil Ostracoda. W. Junk Publishers, The Hague, pp. 395–405.
Krstic, N., Dermitzakis, M.D., 1981. Pleistocene fauna from a section in the channel of Corinth (Greece). Annales Geologiques des Pays Helleniques, 1e Serie 30 (2), 473–499.
Lachenal, A.M., 1989. Ecologie Des Ostracodes Du Domaine Méditerranéen. Application Au Golfe De Gabes (Tunisie Orientale) Les Variations Du Niveau Marin Depuis 30,000 Ans. Doc. Lab. Geol. Lyon, 108, 239pp. .
Leszczyński, S., Kołodziej, B., Bassi, D., Malata, E., Gasiński, M.A., 2012. Origin and resedimentation of rhodoliths in the late paleocene flysch of the polish outer carpathians. Facies 58, 367–387.
Ligios, S., Gliozzi, E., 2012. The genus *Cyprideis* Jones, 1857 (Crustacea, Ostracoda) in the Neogene of Italy: a geometric morphometric approach. Rev. Micropalã©ontologie 55, 171–207.
Loeblich, A.R., Tappan, H., 1988. Foraminiferal Genera and Their Classification. Van Nostrand Reinhold, New York.
Loeblich, A.R., Tappan, H., 1994. Foraminifera of the Sahul Shelf and Timor Sea.Cushman Foundation for Foraminiferal Research Special Publication 31, Washington. .
Mazzini, I., Anadon, P., Barbieri, M., Castorina, F., Ferreli, L., Gliozzi, E., Mola, M., Vittori, E., 1999. Late Quaternary sea-level changes along the Tyrrhenian coast near Orbetello (Tuscany, central Italy): palaeoenvironmental reconstruction using ostracods. Mar. Micropaleontol. 37 (3–4), 289–311.
Mazzini, I., Faranda, C., Giardini, M., Giraudi, C., Sadori, L., 2011. Late Holocene palaeoenvironmental evolution of the Roman harbour of Portus, Italy. J. Paleolimnol. 46, 243–256.
McMurray, L.S., Gawthorpe, R.L., 2000. Along-strike variability of forced regressive deposits: late quaternary, northern peloponnesos, Greece. In: Hunt, D., Gawthorpe, R. L. (Eds.), Sedimentary Responses to Forced Regressions, Geological Society of London Special Publications, 172. , pp. 363–377.
Meisch, C., 2000. Freshwater ostracoda of Western and Central Europe. In: Schwoerbel, J., Zwick, P. (Eds.), Susswasserfauna Von Mitteleuropa, 8/3, , pp. 522.
van Morkhoven, F.P.C.M., 1962. Post-Paleozoic Ostracoda. Their Morphology, Taxonomy and Economic Use. Volume 1, General. Elsevier, Amsterdam, pp. 204.
Mostafawi, N., 1994. Ostracoden aus dem Ober-Pliozän und dem Ober-Pleistozän des N–Peloponnes, Griechenland. Neues Jahrbuch für Geologie und Paläontologie, Abhandlungen 194 (1), 95–114.
Murray, J.W., 1991. Ecology and Paleoecology of Benthic Foraminifera. John Wiley & Sons, New York, pp. 397.
Pallikarakis, A., Triantaphyllou, M., Papanikolaou, I.D., Dimiza, M.D., Reicherter, K., Migiros, G., 2018. Age Constraints and Paleoenvironmental Interpretation of a Borehole Sedimentary Sequence at the Eastern Part of Corinth Isthmus, Greece. J. Coast. Res. 34 (3), 602–617.
Pallikarakis, A., Papanikolaou, I.D., Reicherter, K., Triantaphyllou, M., Dimiza, M.D., Koukousioura, O., 2019. Constraining the regional uplift rate of the Corinth Isthmus area (Greece), through biostratigraphic and tectonic data. Z. Fã¼r Geomorphol. 62 (2), 127–142.
Palyvos, N., Mancini, M., Sorel, D., Lemeille, F., Pantosti, D., Julia, R., Triantaphyllou, M., De Martini, P.M., 2010. Geomorphological, stratigraphic and geochronological evidence of fast Pleistocene coastal uplift in the westernmost part of the Corinth Gulf Rift (Greece). Geol. J. 45 (1), 78–104.
Papadopoulou, P., Iliopoulos, G., Protopapas, D., Spyropoulos, S., Karanika, K., Tsoni, M., Koukouvelas, I., 2019. Formation, evolution and demise of a tectonically controlled volcanic lake: a case study from the lower Pleistocene Sousaki succession. Geobios 55, 41–55.
Papanikolaou, I.D., Triantaphyllou, M., Pallikarakis, A., Migiros, G., 2015. Active faulting at the Corinth Canal based on surface observations, borehole data and paleoenvironmental interpretations. Passive rupture during the 1981 earthquake sequence? Geomorphology 237, 65–78.
Pavlopoulos, K., Karkanas, P., Triantaphyllou, M., Karymbalis, E., Tsourou, T., Palyvos, N., 2006. Paleoenvironmental evolution of the coastal plain of marathon, Greece, during the late holocene: deposition environment, climate and sea-level changes. J. Coast. Res. 22 (2), 424–438.
Pederson, C.L., Mc Neill, D.F., Klauss, J.S., Swart, P.K., 2015. Deposition and diagenesis of marine oncoids: implications for development of carbonate porosity. J. Sediment. Res. 85, 1323–1333.
Perch-Nielsen, K., 1985. Cenozoic calcareous nannofossils. In: Bolli, H.M., Saunders, J.B., Perch-Nielsen, K. (Eds.), Plankton Stratigraphy, 427-554. Cambridge University Press, Cambridge.
Pierini, F., Demarchi, B., Turner, J., Penkman, K., 2016. *Pecten*as a new substrate for IcPD dating: The quaternary raised beaches in the Gulf of Corinth, Greece. Quat. Geochronol. 31, 40–52.
Raffi, I., Backman, J., Fornaciari, E., Palike, H., Rio, D., Lourens, L., Hilgen, F., 2006. A review of calcareous nannofossil astrobiochronology encompassing the past 25 million years. Quat. Sci. Rev. 25 (23), 3113–3137.
Richter, D.K., Sedat, R., 1983. Brackish-water oncoids composed of blue-green and red algae from a pleistocene terrace near corinth, Greece. In: Peryt, T. (Ed.), Coated Grains. Springer, Berlin, pp. 299–307.
Rio, D., Raffi, I., Villa, G., 1990. Pliocene-Pleistocene calcareous nannofossil distribution patterns in the western Mediterranean. Proc. Ocean Drill. Prog. Sci. Results 107, 513–533.
Ruiz, F., Gonzalez-Regalado, M.L., Baceta, J.I., Muñoz, J.M., 2000. Comparative ecological analysis of the ostracod faunas from low- and high-polluted southwestern Spanish estuaries: a multivariate approach. Mar. Micropaleontol. 40 (4), 345–376.
Sgarrella, F., Moncharmont Zei, M., 1993. Benthic foraminifera of the Gulf of Naples(Italy): systematics and autoecology. Boll. Soc. Paleontol. Ital. 32, 145–264.
Shornikov, E.I., 1969. Podklass Ostrakoda, Ili Rakushkovye Raki - Ostracoda latreille (Ostracoda Latreille of the Black Sea). in: Opredelitel' Fauny Chernogo i Azovskogo Morey (A Key to Black Sea and Azov Sea Fauna). Kiev, Naukova Dumka, II, 163-260 (in Russian). .
Thierstein, H.R., Geitzenauer, K.R., Molfino, B., Shackleton, N.J., 1977. Global synchroneity of Late Quaternary coccolith datum levels validation by oxygen isotopes. Geology 5 (7), 400–404.
Triantaphyllou, M., 2015. Calcareous nannoplankton dating of the Late Quaternary deposits in Greece and the eastern Mediterranean: case studies from terrestrial and marine sites. Journal of Paleogeography 4 (4), 1–9.
Triantaphyllou, M.V., Pavlopoulos, K., Tsourou, T., Dermitzakis, M.D., 2003. Brackish marsh benthic microfauna and palaeoenvironmental changes during the last 6.000 years on the coastal plain of Marathon (SE Greece). Rivista Italianna di Paleontologia e Stratigrafia 109 (3), 539–547.
Triantaphyllou, M., Kouli, K., Tsourou, T., Koukousioura, O., Pavlopoulos, K., Dermitzakis, M.D., 2010. Paleoenvironmental changes since 3000 BC in the coastal marsh of Vravron (Attiki, SE Greece). Quat. Int. 216, 14–22.
Tsourou, Th., 2012. Composition and distribution of recent marine ostracod assemblages in the bottom sediments of Central Aegean Sea (SE Andros Island, Greece). Int. Rev. Der Gesamten Hydrobiol. Und Hydrogr. 97 (4), 276–300.
Tsourou, Th., Drinia, H., Anastasakis, G., 2015. Ostracod assemblages from Holocene middle shelf deposits of southern Evoikos Gulf (central Aegean Sea, Greece) and their palaeoenvironmental implications. Micropaleontology 61 (1-2), 85–99.
Yassini, I., Ghahreman, A., 1976. Récapitulation de la distribution des ostracodes et des foraminiféres du lagon de Pahlavi, province de Gilan, Iran du nord. Revue de Micropaléntologie 19, 172–190.
Young, J.R., 1994. Functions of coccoliths. In: Winter, A., Siesser, W.G. (Eds.), Coccolithophores. Cambridge University Press, Cambridge, pp. 63–82.